Sigma Journal of Engineering and Natural Sciences
Web page info: https://sigma.yildiz.edu.tr
DOI: 10.14744/sigma.2022.00099

Research Article

Virtual testing of aluminum and Nomex® honeycomb core structures using ls-dyna and Python/Seaborn

Alparslan SOLAK[1*], Birgül AŞÇIOĞLU TEMIZTAŞ[1], Berna BOLAT[1]

[1]*Department of Mechanical Engineering, Yildiz Technical University, Besiktas, 34349, İstanbul, Türkiye*

ARTICLE INFO

Article history
Received: 11 March 2021
Revised: 15 July 2021
Accepted: 21 September 2021

Keywords:
Compression; Honeycomb; Aluminum; Nomex®; Ls-Dyna; Python/Seaborn

ABSTRACT

Honeycombs are essential elements in mechanical systems where low weight and high strength are required. Aluminum and Nomex® are the most commonly used honeycomb materials in structures exposed to compression stress. The primary purpose of this study is to verify the compression behavior of honeycombs in Ls-Dyna using experimental values and theoretical equations. Additionally, it is aimed to evaluate the honeycombs parameters such as cell diameter, cell wall thickness, and material. A correlation matrix was created using the Python/Seaborn program to examine the impact coefficients of the parameters. In this way, the effect of design parameters on compression strength and internal energy was investigated.

Cite this article as: Solak A, Aşçıoğlu Temiztaş B, Bolat B. Virtual testing of aluminum and Nomex® honeycomb core structures using ls-dyna and Python/Seaborn. Sigma J Eng Nat Sci 2022;40(4):831–844.

INTRODUCTION

Honeycomb materials are widely used in aircraft components, in which the compressive strength/density ratio is crucial for structural integrity and minimization of the weight. These are achieved by the optimum combination of the design parameters using a lot of structural analyses. Cell size, web thickness and material selection are some of the critical parameters in a honeycomb design. Increasing the thickness of the honeycombs increases the strength of the sandwich structure. However, the increase in strength is higher than the rate of increase in weight [1, 2]. The main reason for its frequent use is its flexible structure, simplicity of production, lightness, and high strength [1]. The honeycombs used in different parts of the aircraft are shown in Fig. 1.

Previous experimental, theoretical, and numerical studies have been conducted better to understand the compression behavior of aluminum and Nomex® honeycombs. To illustrate, Gibson and Ashby [2] researched the mechanical behavior of honeycombs. The theoretical equations related to the elasticity modulus of the

***Corresponding author.**
*E-mail address: asolak@yildiz.edu.tr; alparslansolak1992@hotmail.com

This paper was recommended for publication in revised form by Regional Editor Mostafa Safdari Shadloo

honeycomb in the third direction, the shear modulus of the 3-1 and 3-2 planes, and the elastic strength in the third direction were derived. The work of Gibson and Ashby applies to isotropic materials such as aluminum but not to anisotropic materials such as Nomex® material. Folding in aluminum honeycombs is smooth, but the Nomex® honeycombs show uneven folds and break edges. Therefore, aluminum equations cannot be used for Nomex® honeycombs. Zhang and Ashby [3] investigated the mechanical behavior of Nomex® honeycombs in the third direction. In this study, the buckling and fracture caused by compression stress applied in the third direction in honeycombs were explained by theoretical equations. The results were consistent with the experimental values of Nomex® honeycombs. Although theoretical studies showed that materials exhibit isotropic and anisotropic behavior, they may exhibit different behaviors in applications. Therefore, the experimental test results must be used to validate the Ls-Dyna model.

Bitzer [1] mentioned the use of honeycombs as commercial products. The mechanical behavior of honeycombs made of various materials, particularly aluminum and Nomex® honeycombs, was investigated. The theoretical equations of honeycombs produced in hexagonal and various forms were emphasized. Khan [4] carried out several experimental tests following the ASTM C-365 (Standard Test Method for Flatwise Compressive Properties of Sandwich Cores) [5] to be used in the selection of materials for air and space structures. Aluminum honeycomb was tested separately as bare and a sandwich in these tests. Foo et al. [6] investigated the linear elastic properties of Nomex® paper and Nomex® honeycomb with an experimental test setup following ASTM standards. The results obtained were compared with theoretical equations, and the effect of geometric properties on the Nomex® honeycomb elasticity module was investigated.

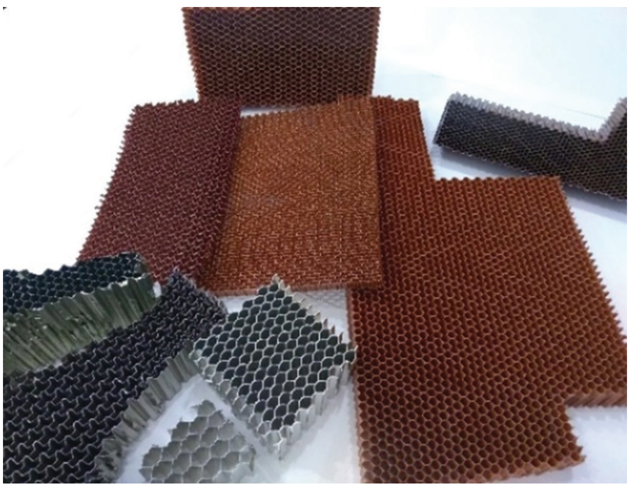

Figure 1. Honeycomb core materials.

Experimental testing of honeycomb structures is time-consuming and expensive. Analysis methods of the finite element have been developed to prevent these costs. Ls-Dyna is a standard program of analysis in this field. The analysis results and the simulations that are very close to the experimental results are given so that they are used as a standard in the development process [7]. In the compression tests of honeycomb materials, Ls-Dyna is generally used before the design to make it easier for the designer while deciding on the parameters. Since this is not sufficient, the correlation among design parameters should be made more explicit using Python code.

Heimbs et al. [7-9] worked on virtual testing of Nomex® and carbon fiber honeycombs. The effects on the analysis of parameters such as material, mesh size, and cell geometry was emphasized. Shell and solid elements were used in the studies. For these models, MAT54 and MAT126 material cards were used in Ls-Dyna. The numerical and experimental studies were compared to validate the models. Seemann and Krause [10,11] focused on the honeycomb, which was made of Nomex® T-412. In this study, 4 different Nomex® honeycomb models were used in the finite element environment. It was stated that the single-layer orthotropic approach among these models is the most recommended model because it reflects the experimental tests well. In comparison to the actual experimental tests, the model was reduced to 8 cells, in which the time of analysis was reduced and savings were made. Meran et al. [12] studied the crash resistance parameters for aluminum honeycombs. These parameters included cell wall thickness, cell diameter, cell opening angle, impact speed, and mass. Experimental testing was performed, and theoretical equations were used to verify the finite element model. Roy et al. [13] determined the mechanical properties of Nomex® paper for use in finite element models. As an experimental test, the tensile test of Nomex® paper and tensile-compression tests of honeycomb made of Nomex® material were performed. While modeling honeycomb in hexagonal form, non-stick parts were modeled as one unit, and the sticky parts were modeled in two units. Xie et al. [14] studied the mechanical behavior of the sandwich structure under impact load. The core material of the sandwich structure was Nomex®. Considering the density of the honeycomb, the thickness of the surface plates, the diameter of the impact part, the energy parameters of the impact, and the damage modes in the sandwich structure were examined. Their experimental values and numerical values were compared.

There are many studies in the literature on the analysis of honeycomb using Ls-Dyna. Also, there are different areas where the Python/Seaborn program is used. However, there is no study evaluating honeycomb parameters using Ls-Dyna and Python/Seaborn together. Using these two together, we aim to understand the relationship between design parameters using the results from Ls-Dyna with Python/Seaborn. Also, it is to create a reference source for future optimization and design improvement studies. In this research, compression test models of aluminum and Nomex® honeycombs in Ls-Dyna were established in section 2. MAT18, MAT26 and MAT54 material cards were used in Ls-Dyna. Different mesh sizes and compression head speeds were used to approach experimental data. These experimental data are the breaking behavior and the highest compressive strength. The results of the Ls-Dyna model yielded to be compatible with experimental and theoretical calculations. After verification, a series of analyses were performed for different cell sizes and cell wall thicknesses. A structural analysis database was built in the design tool by taking permutations of the parametric variables. In section 3, with this database, the correlation matrix was established using Python/Seaborn [15] program based on the data analysis approach. In this way, the relationship between the parameters affecting the thirty-two Ls-Dyna analysis results was understood. In section 4, the comparison of aluminum and Nomex® honeycomb and the parameter impact coefficients were mentioned. In the last section, the benefit of using Ls-Dyna and Python/Seaborn together, and recommendations for future work were discussed.

NUMERICAL MODELING USING LS-DYNA

Experimental values and theoretical formulas were used to validate the Ls-Dyna models. In this way, the largest elastic compression strength values of the models were compared.

Aluminum Honeycomb

Fig. 2 shows the structure descriptions of the aluminum model in Ls-Dyna. In Fig. 2(a), the yellow shows double-thickness and grey represents single-thickness. Fig. 2(b) shows the geometrical expressions of this honeycomb. Fig. 2(c) shows the test sample. The directions W and L represent the directions of the plane, and T represents the normal direction of the plane. Also, D is the cell diameter, l is the one side of the cell, t is the single layer of the cell wall, 2t is the double cell wall, Θ is the expansion angle and h is the core thickness.

The geometric properties and strength value of the honeycomb which were collected from this experiment were given in Table 1.

A theoretical comparison was based on Gibson and Ashby's theoretical equation. Maximum strength calculation that can be applied elastically in aluminum honeycombs [2].

$$(\sigma_{el}^{3}) = 5.2E_{s}(t/l)^{3} \tag{1}$$

In this equation, σ_{el}^{3} represents the highest elastic compressive strength in the 3rd direction, is the modulus of material elasticity, t is the cell wall thickness of the honeycomb, and l is the length of the hexagonal side of the honeycomb. The theoretical compressive strength value is 1.95 MPa when the features given in Table 1 are applied in Eq. (1).

The finite element model in the compression test established for numerical analysis is shown in Fig. 3. According

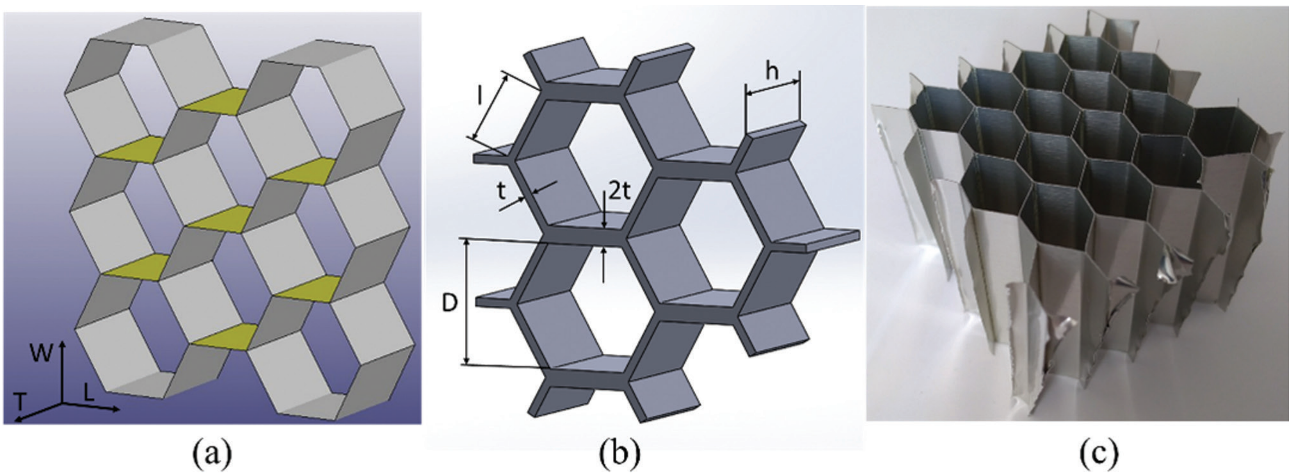

Figure 2. Honeycomb core materials (a) The surfaces of honeycomb, (b) geometrical dimensions, (c) test sample.

Table 1. Geometric and mechanical properties of honeycomb [4]

Material	Elasticity module (GPa)	Cross-section area (mm²)	Core thickness (mm)	Cell size (mm)	Web thickness (mm)	Experimental strength (MPa)
Al 3003	68.94	33.5x62.4	10.2	6.3	0.064	2.15

to the ASTM C-365 [5] standard, 60 cells were drawn in the ANSYS Workbench module using the Honeycomb-Creator [24] extension and transferred to Ls-Dyna using the .step extension.

In the experimental tests, since the compression head is more challenging than the honeycomb, the head was considered rigid in the finite element environment. For this case, PLANAR_MOVING_FORCES in the RIGIDWALL model [27, 28, 29] was selected. The head speed should be 0.5 mm/min according to ASTM C-365 [5] standard. Due to the nature of finite elements, the resolution time in quasi-static loadings is not acceptable due to such speeds [9]. The head speed can be increased to shorten the time required for the solution. Therefore the head speed was increased in the Ls-Dyna finite element model. The shell element Belytschko-Tsay was selected for the structure of the cell walls in the honeycomb [7]. For the aluminum 3003 [25, 26] material model, MAT18-POWER_LOW_PLASTICITY was chosen. Table 2 shows the parameters for the material model.

The AUTOMATIC_SINGLE_SURFACE [14, 19, 20, 22, 30] contact has been defined between the honeycomb walls. In this way, unrealistic interlacing among shell elements was prevented. The head under the honeycomb was fixed during the experiment, and the upper part of the honeycomb moves downward with the head. For boundary conditions in the Ls-Dyna environment, 6 degrees of freedom of the nodes at the lower edges of the honeycomb were limited [10]. Constrained nodes are shown in red and unconstrained nodes are shown in green (Fig. 4).

The selection of mesh sizes is essential [7]. Too small mesh size lengthens the analysis time excessively. Incorrect mesh size similarly causes deviation from experimental values. In an experiment, Khan found the aluminum honeycomb's compressive strength to 2.15 MPa [4]. In this study, five different mesh sizes were tested by applying 0.5 m/s speed to approximate the experimental value. The size of the mesh used varies from 0.4 mm to 1.82 mm. Ls-Dyna compression test results for various mesh sizes are shown in Fig. 5.

The result of the 1.21 mm mesh size shown in Fig. 5 is closer to the 2.15 MPa experimental test value than the

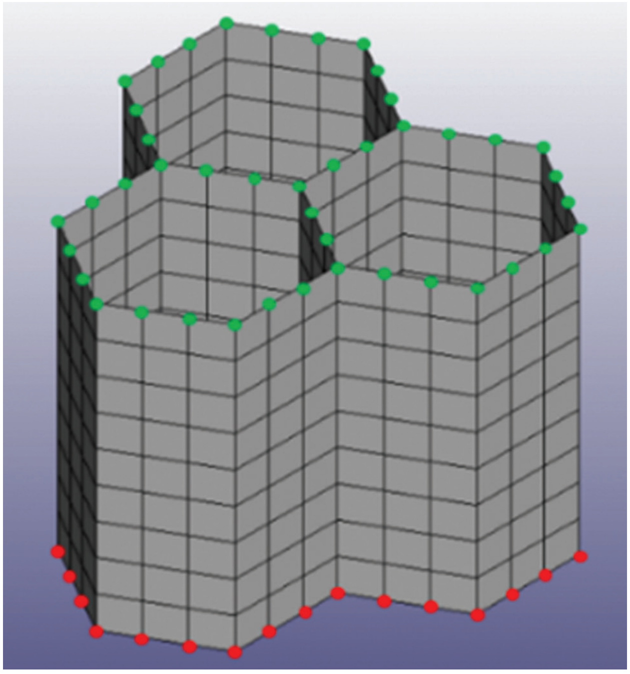

Figure 4. Restricted and free nodes with 6 degrees of freedom.

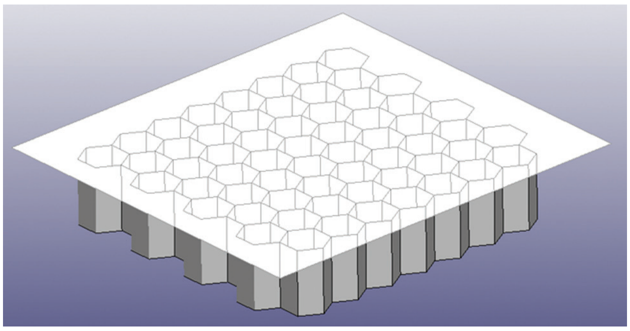

Figure 3. Ls-Dyna finite element model for aluminum honeycomb.

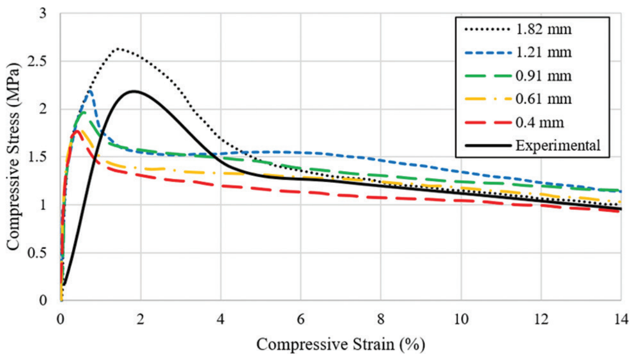

Figure 5. Mesh sizes and Ls-Dyna compression test results.

Table 2. Material parameters for MAT18

Mass density (RO)	Young's modulus (E)	Poisson's ratio (PR)	Strength coefficient (K)	Hardening exponent (N)
2.74e-06	68.94	0.33	0.20546	0.2687710

others. Therefore, analyses were made with this mesh size for aluminum. In order to verify the model with the experimental test value, a quasi-static analysis was performed at different speeds for a mesh size of 1.21 mm and is shown in Table 3.

Since the compression speed of 0.5 m/s is closer to the experimental test value compared to other speeds, the aluminum analyses were performed at this speed. The internal energy changes are similar to each other at speeds up to 1 m/s of the head. However, as the speed increases, the amount of internal energy change also increases. This shows us that the speed selection of the compression head is important and the value should be chosen as close to ASTM as possible.Theoretical, experimental and Ls-Dyna finite element model results are shown in Table 4.

According to Table 4, there is a 10.1% difference between the Ls-Dyna model and the theoretical calculation. In addition, there is a 0.92% difference between the Ls-Dyna model and the experimental test value. A close relationship was observed between the Ls-Dyna analysis result and the experimental result.

The compression behavior and stages of the aluminum honeycomb in Ls-Dyna are shown in Fig. 6. When Ɛ=0.74, the highest elastic strength value is 2.17 MPa. Up to this point, the aluminum honeycomb is elastically compressed. When the compressive strain is between Ɛ=0.74 and Ɛ=65, the region is defined as the plateau region. There is plastic folding on the edges of the honeycomb in this region. From the Ɛ=65, plastic folding ended on the edges and the densification zone begins. The folded edges in this area are compressed by the movement of the head, which causes an increase in compression stress.

The steps of the aluminum honeycomb during gradual compression are shown in Fig. 7.

In order to see the effect of cell diameter and cell wall thickness on the highest compressive strength and internal energy, a series of analyses with different values were carried out. The results of the analysis are shown in Table 5. Code was made for modeled aluminum honeycombs. The catalog of the Hexcel firm [18] was used for coding. In the MAT18_1/8_0.001 model, MAT18 is an aluminum

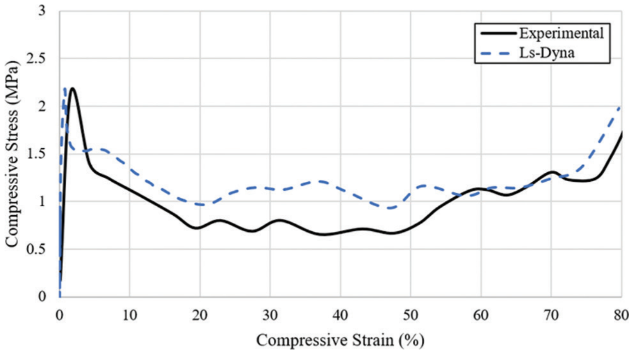

Figure 6. Experimental and Ls-Dyna (1.21 mm mesh size) stress-strain curves for aluminum honeycomb.

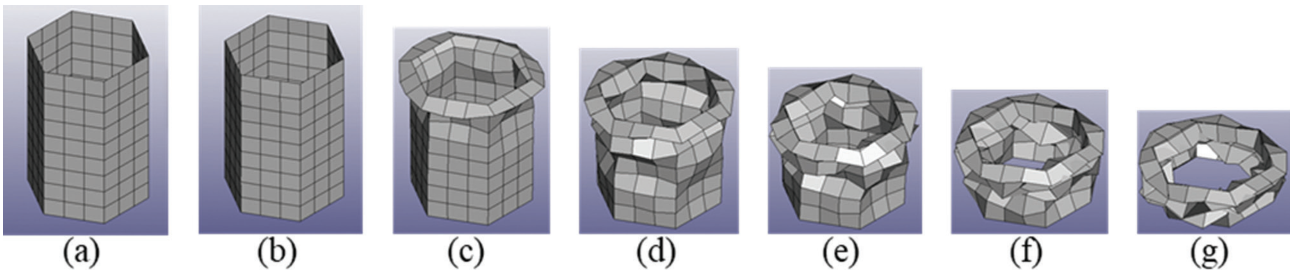

Figure 7. The phases of the aluminum honeycomb model with a mesh size of 1.21 mm during compression.

Table 3. Compressive strengths and internal energies at different speed values

Speed (m/s)	0.25	0.3	0.4	0.5	0.6	0.7	1	2	5
Compressive strength (MPa)	2.01	2.05	2.11	2.17	2.21	2.26	2.37	2.65	3.1
Internal energy (J)	1.39	1.40	1.43	1.43	1.43	1.45	1.47	1.60	2.04

Table 4. Comparison of aluminum honeycomb models for theoretical, experimental and Ls-Dyna

Model type	Theoretical	Experimental	Ls-Dyna model
Compressive strength (MPa)	1.95	2.15	2.17

material model, with 1/8 cell diameter and 0.001 cell wall thickness in inches.

The results given in Table 5 are given in Fig. 8 as a counter with using Minitab program [23]. As shown in Fig. 8, as the cell size increases, the strength value decreases. However, as the wall thickness increases, the strength increases.

Nomex® Honeycomb

Comparison with experimental and theoretical results was made to validate the Nomex® model in Ls-Dyna. Heimbs [7] carried out a series of experimental tests and Ls-Dyna finite element analysis using the commercial product Cormaster C1-3.2-48 honeycomb (Fig. 9) Nomex® material. The compressive strength in the T direction of the regular hexagonal honeycomb was examined in these tests.

The cell diameter of C1-3.2-48 shown in Fig. 9 is 3.2 mm and the cell wall thickness is 0.0613 mm. T-412 aramid paper is a compressed honeycomb wall material. The maximum elastic strength obtained experimentally is 1.94 MPa [21]. The parameters used for the Nomex® model in Ls-Dyna are shown in Table 6 [6,10,11,13,17].

In the Nomex® model, Eq. (2) was derived from Zhang and Ashby [3]. This equation was used to determine the maximum theoretically applicable compressive strength.

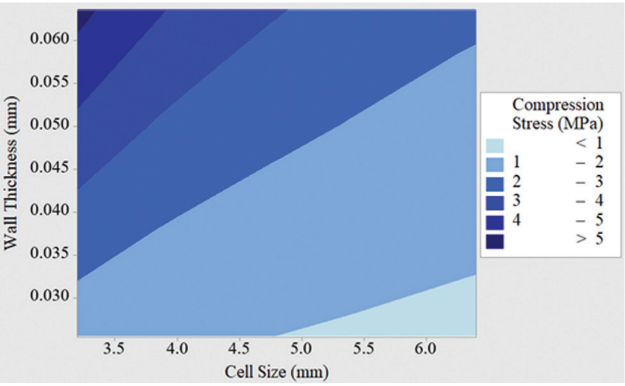

Figure 8. Aluminum honeycomb compressive strength values corresponding to cell size and cell wall thickness.

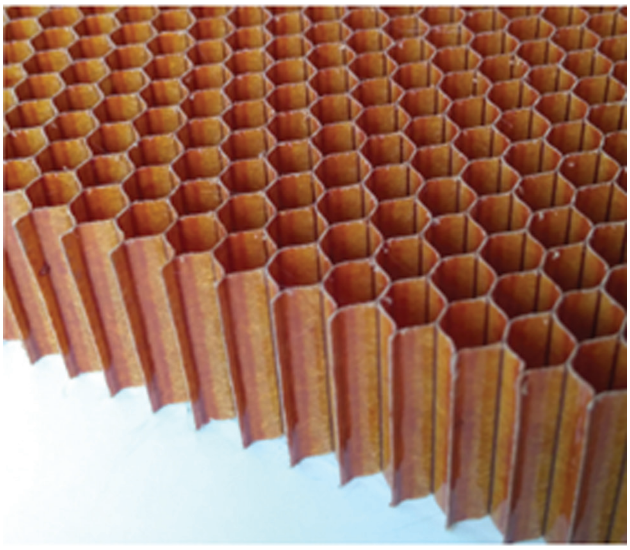

Figure 9. Nomex® honeycomb.

Table 5. Analysis results of aluminum honeycombs

Cell size (mm)	Cell wall thickness (mm)	Compression Strength (MPa)	Internal Energy (J)	Code
3.2	0.0254	1.23	1.521	MAT18_1/8_0.001
3.2	0.0381	2.58	3.055	MAT18_1/8_0.0015
3.2	0.0508	3.59	5.306	MAT18_1/8_0.002
3.2	0.0635	4.37	8.29	MAT18_1/8_0.0025
4	0.0254	0.85	1.704	MAT18_5/32_0.001
4	0.0381	1.71	3.386	MAT18_5/32_0.0015
4	0.0508	2.83	5.927	MAT18_5/32_0.002
4	0.0635	3.63	8.663	MAT18_5/32_0.0025
4.8	0.0254	0.65	1.927	MAT18_3/16_0.001
4.8	0.0381	1.26	3.83	MAT18_3/16_0.0015
4.8	0.0508	2.20	6.259	MAT18_3/16_0.002
4.8	0.0635	2.97	9.575	MAT18_3/16_0.0025
6.4	0.0254	0.47	2.247	MAT18_1/4_0.001
6.4	0.0381	0.87	4.518	MAT18_1/4_0.0015
6.4	0.0508	1.38	7.129	MAT18_1/4_0.002
6.4	0.0635	2.09	10.155	MAT18_1/4_0.0025

$$\sigma_T \approx 6E_s\,(\rho/\rho_s)^3 \quad (2)$$

In this equation, the expression σ_T represents the highest elastic compressive strength in the 3rd direction. E_s represents the elasticity module of the Nomex® material in the machine direction, ρ represents the density of the Nomex® honeycomb and ρ_s represents the density of the Nomex® paper. The theoretical compressive strength value is 2.39 MPa when the features given in Table 6 are applied in Eq. (2).

There are many methods in the literature for modeling Nomex® honeycomb. Analyses were performed using a single layer orthotropic approach (Fig. 10) [10] because it is compatible with the test results and the time required for analysis solution time is short.

The minimum number of cells to be tested should be 60 cells according to the ASTM C-365 standard [5]. However, making 60 cells like the actual experimental test increases analysis time. Therefore, the sample was shrunk and modeled as 8 cells in Ls-Dyna (Fig. 11) [11].

Due to the downward movement of the head in the model, compression stress occurs in the Nomex® honeycomb. PLANAR_MOVING_FORCES was selected for the head in the RIGIDWALL model. The Belytschko-Tsay shell element was chosen for the modeling of cell walls [7]. Unlike aluminium, Nomex® paper is not a mechanically isotropic material. It has different mechanical properties in the direction of the machine and in the direction of the cross. An orthotopically elastic-perfect plastic composite material model is required for these properties. Since the cell wall material is unidirectional, MAT054/055-ENHANCED_COMPOSITE_DAMAGE was chosen [7]. AUTOMATIC_SINGLE_SURFACE contact was defined in

Table 6. Primary parameters for Nomex® wall paper

Definition	Parameter	Unit	Value
Mass density	(RO)	kg/(m^3)	940
Young's modulus-longitudinal direction	(EA)	GPa	3
Young's modulus-transverse direction	(EB)	GPa	1.7
Young's modulus-normal direction	(EC)	GPa	1.7
Poisson's ratio ba	(PRBA)	-	0.2
Poisson's ratio ca	(PRCA)	-	0.2
Poisson's ratio cb	(PRCB)	-	0.3
Shear modulus ab	(GAB)	GPa	1.2
Shear modulus bc	(GBC)	GPa	1.2
Shear modulus ca	(GCA)	GPa	1.028
Longitudinal compressive strength	(XC)	MPa	45
Longitudinal tensile strength	(XT)	MPa	90
Transverse compressive strength	(YC)	MPa	30
Transverse tensile strength	(YT)	MPa	60
Shear strength, ab plane	(SC)	MPa	55
Failure criterion	(CRIT)	-	55

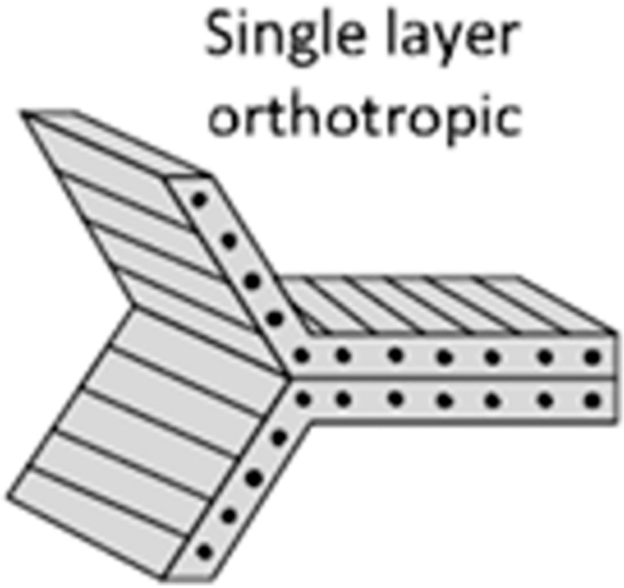

Figure 10. Single-layer orthotropic approach [10].

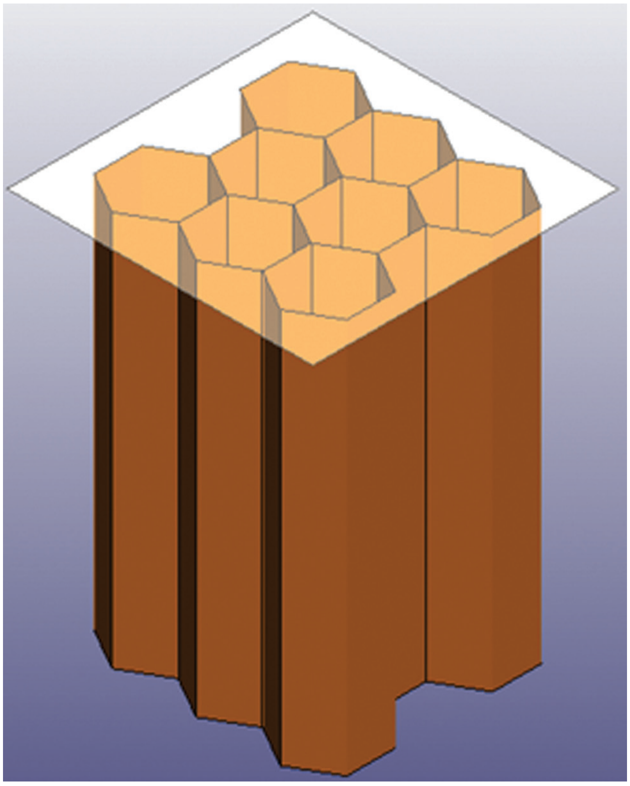

Figure 11. Ls-Dyna finite element model for Nomex® honeycomb.

the Nomex® honeycomb model to prevent cell walls from passing through each other. Some factors should be examined in Ls-Dyna to approach experimental test results [7]. These factors are the model of the cell wall material, the speed of the head and the mesh size. In order to get closer to the actual result, the fracture behavior and the compressive strength value were checked. The experimental fracture behavior of the honeycomb C1-3.2-48 Nomex® is shown in Fig. 12.

The fracture behavior of Nomex® honeycombs with different mesh sizes is shown in Fig. 13.

The experimental maximum compression test value for honeycomb C1-3.2-48 Nomex® is 1.94 MPa. The mesh size closest to this value is 0.46 mm. The fractures in the Nomex® honeycomb are seen to be in the middle of the test sample when the experimental test is examined. The only model in which the fracture can be seen in the middle is the 0.46 mm mesh size model. For these reasons, this mesh size was selected for analysis. The effect of different mesh sizes on compression stress can be seen in Fig. 14.

Heimbs et al. studied the compressive stress-compressive strain behavior of Nomex® honeycomb at different compression speeds [9]. Different compressive strength values were achieved at different speeds. In this case, the experimental strength value and the buckling of the Nomex® honeycomb cell walls must be precisely simulated. A series of Ls-Dyna analyses were conducted at different speeds to approximate experimental values in the Heimbs et al. study. In the analyses, 1.92 MPa was detected at 0.7 m/s. Results are presented in Table 7.

Similar to aluminum honeycombs, compression speed is an effective factor in Nomex® honeycombs. To obtain more accurate values, it is necessary to apply ASTM standards. Theoretical, experimental and Ls-Dyna finite element model results are shown in Table 8.

According to Table 8, there is a 19.6% difference between the Ls-Dyna model and the theoretical calculation. Also, there is a 1.03% difference between the Ls-Dyna

Figure 12. Experimental fracture of C1-3.2-48 Nomex® honeycomb [8].

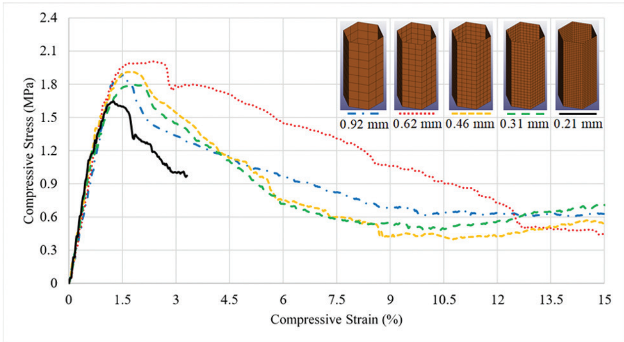

Figure 14. Compressive stress-compressive strain for different mesh sizes.

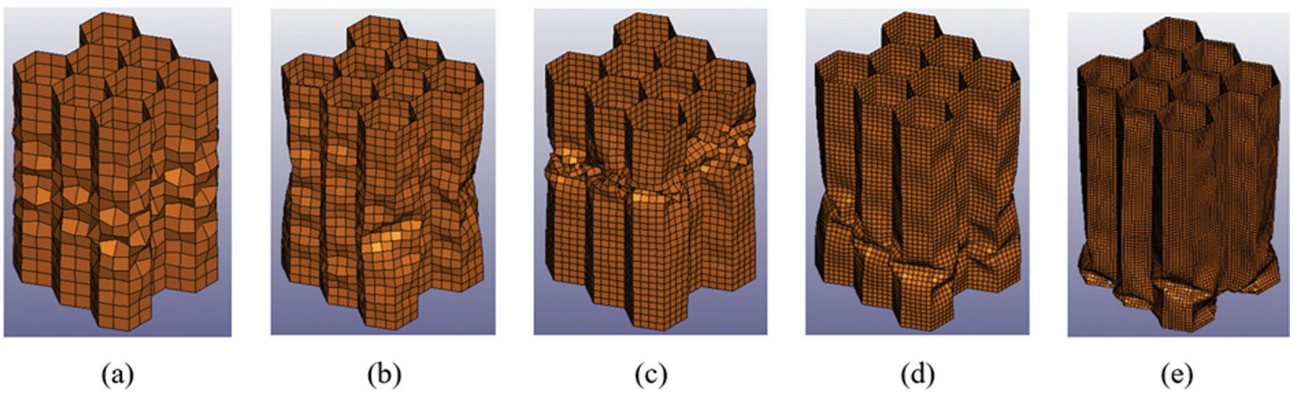

Figure 13. Different mesh sizes and fracture behaviors a) 0.92mm, b) 0.62mm, c) 0.46mm, d) 0.31mm, e) 0.21mm.

Table 7. Nomex® honeycomb strength values at different compression speeds

Speed (m/s)	0.25	0.3	0.4	0.5	0.6	0.7	1	2	5
Compressive strength (MPa)	1.9	1.9	1.9	1.92	1.92	1.9	2.06	2.45	2.71
Internal energy (J)	0.12	0.12	0.12	0.13	0.13	0.13	0.14	0.16	0.18

model and the experimental test value. Close harmony is observed between the result of the Ls-Dyna analysis and the experimental result.

The experimental test, the analysis of Ls-Dyna in the Heimbs study [21], and the Ls-Dyna analysis results within the scope of this research are shown in Fig. 15. The strength value of the two Ls-Dyna models is compatible with the highest experimental compressive strength value. On the other hand, there is a difference between the models and the experimental graphic for the plateau region. The highest compression value was obtained using a single-layer orthotropic approach in a finite element analysis, but there are differences in the plateau region [10]. The densification region of the models and the curves of the densification regions in the experimental test are parallel to each other.

The fracture behaviors in Ls-Dyna are shown in Fig. 16 for the different compressive strain values of the Nomex® honeycomb during the compression test. The highest compressive strength value (1.92 MPa) was found for ε=1.67. Buckling occurs in the cell walls during this compressive strain value. Folding and crushing were observed at ε=15 and other increasing values.

In order to see the effect of cell diameter and cell wall thickness on the highest compressive strength and internal energy, a series of analyses with different values were conducted. The results of the series of analyses are shown in Table 9. The catalog of the company Schütz [16] was used for coding. In the MAT54_1/8_0.001 model, MAT54 is Nomex® material model, 1/8 cell diameter and 0.001 cell wall thickness in inches.

Table 8. Comparison of Nomex® honeycomb models for theoretical, experimental and Ls-Dyna

Model Type	Theoretical	Experimental	Ls-Dyna model
Compressive strength (MPa)	2.39	1.94	1.92

The values obtained in Table 9 are shown in Fig. 17 in three dimensions using Minitab program [23]. Similar to the aluminum results, the strength decreases as the size of the cells increases, but the strength increases as the thickness of the wall increases.

MAT26 Nomex® honeycomb model

Deformation can be reasonably estimated if the shell element is used in the small size of the Nomex® honeycomb model [8]. However, the shell element is not appropriate because the calculation time was long in large-scale models. In this case, the MAT26-HONEYCOMB [31] material model is defined for the solid elements to maintain homogeneity and to be resolved in a shorter time. Fig. 18 shows the Nomex® honeycomb model in which MAT26 material model was defined in Ls-Dyna.

For the mechanical properties of the Nomex® C1-3.2-48 honeycomb, 6 graphs must be defined in the MAT26 material model. Experimentally obtained 3 compressive stress-compressive strain graphs (T, W and L directions) and 3 shear stress-strain graphs (LT, WT and LW planes) were defined [8].

Mesh size is essential in this part as well. For the LW plane, solid elements with a size of 2 mm were used in the model shown in Fig. 18. Only the mesh sizes of the elements

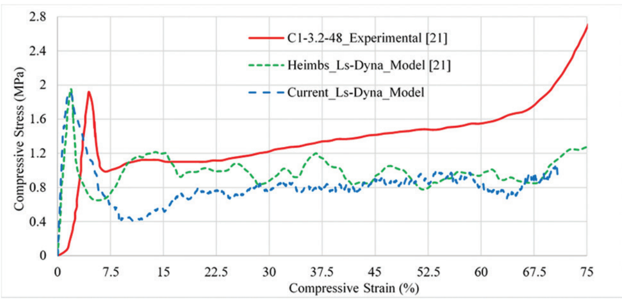

Figure 15. Comparison of experimental and Ls-Dyna results for the compression behavior of Nomex® honeycomb.

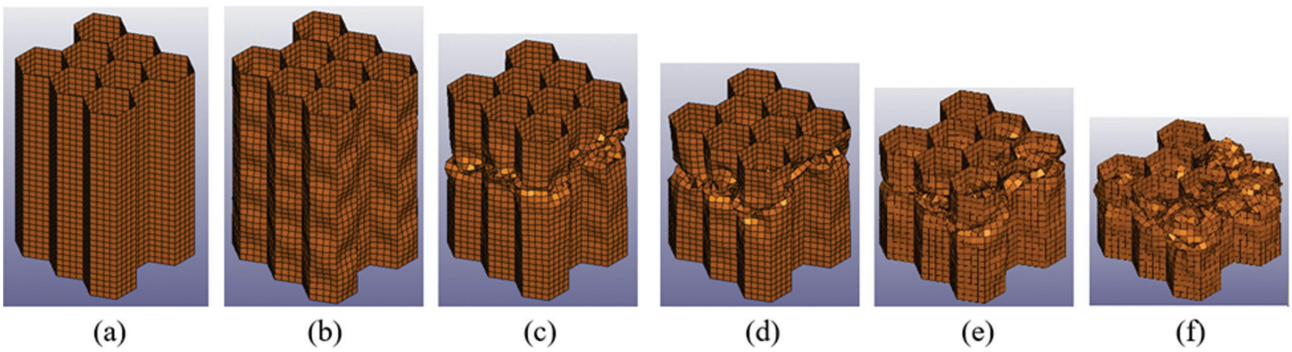

Figure 16. The phases of the Nomex® honeycomb model with a mesh size of 0.46 mm during compression a) ε=0, b) ε=1.67, c) ε=15, d) ε=30, e) ε=45, f) ε=60.

Table 9. Analysis results of Nomex® honeycombs

Cell size (mm)	Cell wall thickness (mm)	Compression Strength (MPa)	Internal Energy (J)	Code
3.2	0.0254	0.45	0.029	MAT54_1/8_0.001
3.2	0.0381	0.88	0.061	MAT54_1/8_0.0015
3.2	0.0508	1.4	0.100	MAT54_1/8_0.002
3.2	0.0635	2.03	0.142	MAT54_1/8_0.0025
4	0.0254	0.31	0.030	MAT54_5/32_0.001
4	0.0381	0.61	0.066	MAT54_5/32_0.0015
4	0.0508	0.98	0.108	MAT54_5/32_0.002
4	0.0635	1.42	0.157	MAT54_5/32_0.0025
4.8	0.0254	0.24	0.031	MAT54_3/16_0.001
4.8	0.0381	0.47	0.068	MAT54_3/16_0.0015
4.8	0.0508	0.76	0.115	MAT54_3/16_0.002
4.8	0.0635	1.08	0.169	MAT54_3/16_0.0025
6.4	0.0254	0.18	0.036	MAT54_1/4_0.001
6.4	0.0381	0.32	0.075	MAT54_1/4_0.0015
6.4	0.0508	0.51	0.120	MAT54_1/4_0.002
6.4	0.0635	0.69	0.179	MAT54_1/4_0.0025

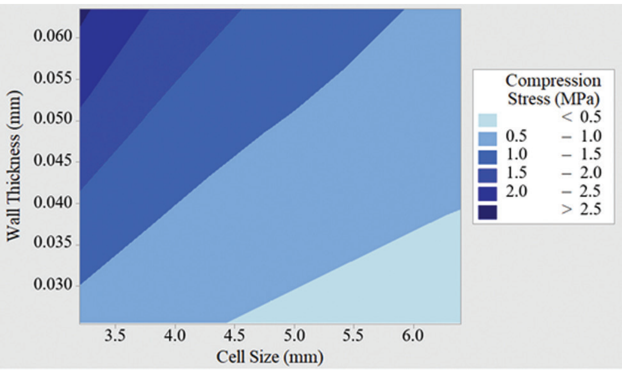

Figure 17. Nomex® honeycomb compressive strength values corresponding to cell size and cell wall.

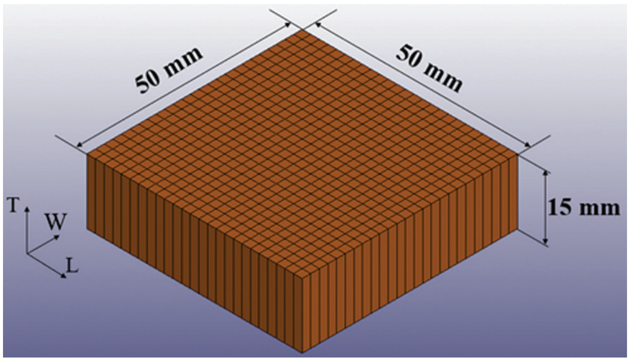

Figure 18. MAT26 Nomex® honeycomb model.

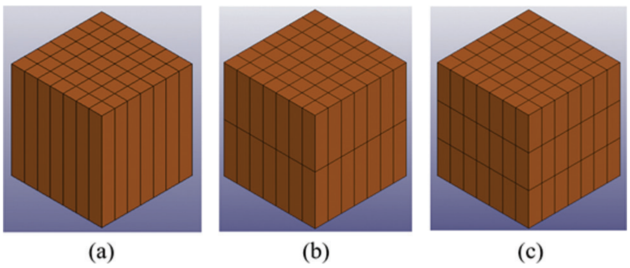

Figure 19. Different mesh sizes a) 15mm, b) 7.5mm, c) 5mm.

in these directions do not have much effect on the result. However, the direction of the T is crucial for this model. As the mesh size changes in the direction of T, the compressive stress-compressive strain curve pattern changes and the maximum elastic strength value changes. Different mesh sizes were used for approximation to experimental value (Fig. 19).

Considering the analysis results in Fig. 20, the elastic compression and densification regions in all 3 models are consistent with the experimental results. Only the 15 mm mesh size model fits the region of the plateau. As the number of elements increases, the number of waves in the region of the plateau increases. There is also a deviation from experimental values.

As seen in Fig. 20, when the highest elastic compressive strength values are compared, the model's value with a mesh size of 15 mm is 1.85 MPa. There is a 4.63% difference with the experimental value (1.94 MPa). Compared

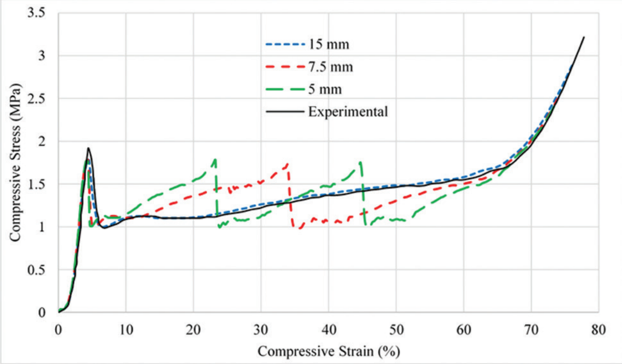

Figure 20. Compression test results of MAT26 Nomex® honeycomb model for different element sizes.

Table 10. Compressive strength values of mesh sizes

Mesh size (mm)	15	7.5	5
Compressive strength (MPa)	1.85	1.78	1.77

with the plateau region and the maximum elastic strength, this model is better suited than the other models. The compressive strength values of different mesh sizes are shown in Table 10.

Creating a matrix of correlation with Python/Seaborn

Bitzer derived Eq. (3) for the density of honeycomb [1]. HD is the density of the honeycomb, ϴ is the angle of expansion, a and b are the sides of the hexagon. Since regular hexagons are used in applications, ϴ=60° and a=b are used.

$$HD = [2(b + a)t\rho]/[(b + a\cos\theta)(2a\sin\theta)] \qquad (3)$$

Using this expression, a comparison was made between the Ls-Dyna analysis results for aluminum and Nomex® honeycombs (Fig. 21). The compressive strength also increases as the density of the aluminum and Nomex® honeycomb increases. As cell diameter increases, the compressive strength/density value of the honeycomb increases.

When compared in terms of compressive strength/density, Nomex® honeycombs show higher performance than aluminum honeycombs. It is seen that as the density of the honeycomb increases, the difference increases.

A correlation matrix was created using the Seaborn Library [15] in the Python program to compare the compressive strength/density results of the aluminum and Nomex® honeycombs, and the correlation coefficients of the parameters among themselves are shown in Fig. 22. In this way, the results of many analyses that are not carried out can be estimated by making a small number of analyses. If the coefficient is 1 according to this matrix, the linear relationship is entirely positive. If the coefficient is 0, there

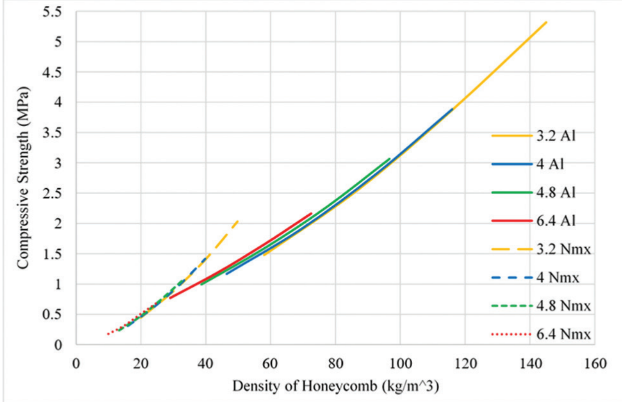

Figure 21. Comparison of aluminum and Nomex® honeycombs.

is no relationship between the two parameters. If the coefficient is -1, there is an entirely negative linear relationship.

The parameters given in Fig. 22 listed in descending order according to the effect size are as follows: Cell wall thickness, cell size, and material. These parameters are 0 in the intersecting rows and columns. In other words, the three parameters are independent of each other. Wall thickness is the parameter that most positively affects the compression strength. Cell size, on the other hand, affects the compressive strength tending to decrease. Because as the cell size increases, the compressive strength decreases. Aluminum material is the parameter that affects the internal energy most positively. On the other hand, the effect of Nomex® material is the lowest. The second most important parameter affecting the internal energy is the wall thickness. The material parameter is not a numeric parameter, unlike cell size and cell wall thickness. Since the material parameter is a verbal expression, it is categorically named in the literature [15]. Therefore, the sign of aluminum is positive as its effect is better than Nomex®. Also, the sign of Nomex® is negative because the effect of Nomex® is not as good as aluminum.

RESULTS AND DISCUSSION

This study focused on the modeling of aluminum and Nomex® honeycombs in the finite element environment. There is an agreement between the values of experimental, theoretical and Ls-Dyna. There is a 0.92% difference between the MAT18 aluminum model and the experimental value for compressive strength. Additionally, there is a 1.03% difference between the MAT54 Nomex® model and the experimental value. There is a 4.63% difference between the MAT26 Nomex® model and the experimental value. Since the MAT26 model has a homogeneous structure and shortens the solution time, it can be used in larger structures, unlike the MAT54 model.

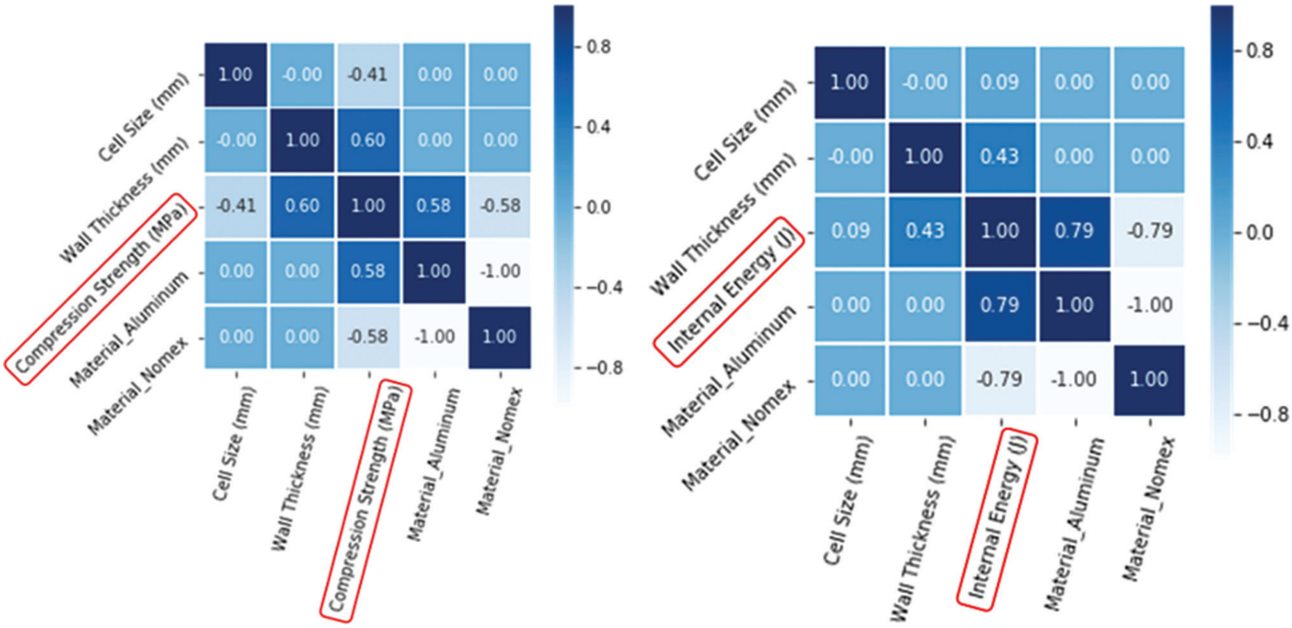

Figure 22. Correlation matrix for parameters.

When the Nomex® honeycomb values are evaluated, although the experimental and Ls-Dyna result graphs are parallel at the plateau region, there is a difference between them. This difference can be overcome by improving the model for future studies. When the same geometries are used as the basis, the aluminum honeycomb has a higher compressive strength than the Nomex® honeycomb. However, the specific strength value "compressive strength/density" must be considered during design. According to this ratio, the Nomex® honeycombs are stronger than the aluminum honeycombs.

In order to understand the effect of the parameters, a series of analyses of aluminum and Nomex® honeycombs with different cell sizes and cell wall thickness were performed. According to these analyses, the strength increases as the cell wall thickness increases, and the strength decreases as the cell size increases. The higher the wall thickness and cell diameter, the higher the internal energy change of the honeycomb during compression. The energy absorption capacity of aluminum is higher than Nomex®. The correlation matrix was created with Python/Seaborn by using the obtained analysis results and the impact coefficients of the parameters were examined. According to this matrix, the parameter that most affects the compression strength is the wall thickness, while the parameter that most affects the internal energy is the aluminum material.

CONCLUSION

In this study, Ls-Dyna models of aluminum and Nomex® honeycombs during compression fit well with experimental and theoretical approaches. Ls-Dyna and Python/Seaborn were used together to understand the effect of design parameters. The main results from this study were given below. In order to verify the Ls-Dyna models, two experimental tests were examined, but 32 different Ls-Dyna analyses were carried out. So, without having to run 30 experimental tests, the same result could be achieved. In addition, the parameters and results of 32 Ls-Dyna analyses were compared with Python/Seaborn. In this way, many results of analysis become predictable without an additional analysis in Ls-Dyna. In future studies, Ls-Dyna and Python/Seaborn programs can be used together in sandwich structures where honeycombs are an element. In this way, the effect coefficients between the parameters of the sandwich structure are revealed. The relationship between the parameters is understood. Based on these coefficients, optimization and improvement studies can be made according to the model's intended use.

ACKNOWLEDGMENT

This research did not receive any specific grant from funding agencies in the public, commercial, or non profit sectors. The authors would like to thank data scientist Orhan Solak for his contribution to the work of Python/Seaborn.

AUTHORSHIP CONTRIBUTIONS

Alparslan Solak: Formal analysis, Validation, Investigation, Writing - original draft. **Birgül Aşçıoğlu Temiztaş:** Methodology, Conceptualization, Supervision, Project administration. **Berna Bolat:** Writing - review & editing, Software, Data curation, Resources, Visualization.

DATA AVAILABILITY STATEMENT

The authors confirm that the data that supports the findings of this study are available within the article. Raw data that support the finding of this study are available from the corresponding author, upon reasonable request.

CONFLICT OF INTEREST

The author declared no potential conflicts of interest with respect to the research, authorship, and/or publication of this article.

ETHICS

There are no ethical issues with the publication of this manuscript.

The authors declare that they have no known competing financial interests or personal relationships that could have appeared to influence the work reported in this paper.

REFERENCES

[1] Bitzer T. Honeycomb Technology. 1st ed. Berlin:Springer Dordrecht;1997. [CrossRef]

[2] Gibson LJ. Ashby MF. Cellular Solids: Structure and Properties. 2nd ed. Cambridge: Cambridge University Press;2014.

[3] Zhang J, Ashby MF. The out-of-plane properties of honeycombs. Int J Mech Sci 1992;34:475–489. [CrossRef]

[4] Khan MK. Compressive and lamination strength of honeycomb sandwich panels with strain energy calculation from ASTM standards. Proc Inst Mech Eng G J Aerosp Eng 2006;220:375–386. [CrossRef]

[5] ASTM. ASTM C365 / C365M-16. Standard Test Method for Flatwise Compressive Properties of Sandwich Cores. West Conshohocken, PA: ASTM International;2016 Avaliable at: https://www.astm.org/c0365_c0365m-16.html Accessed on Nov 02,2022.

[6] Foo CC, Chai GB, Seah LK. Mechanical properties of Nomex material and Nomex honeycomb structure. Compos Struct 2007;80:588–594. [CrossRef]

[7] Heimbs S. Virtual testing of sandwich core structures using dynamic finite element simulations. Comput Mater Sci 2009;45:205–216. [CrossRef]

[8] Heimbs S, Middendorf P, Maier M. Honeycomb sandwich material modeling for dynamic simulations of aircraft interior components. In: editors. 9th International LS-DYNA Users Conference; 2006 June; Dearborn,USA:Publisher; 2006. pp.

[9] Heimbs S, Middendorf P, Kilchert S, Johnson AF, Maier M. Experimental and numerical analysis of composite folded sandwich core structures under compression. Appl Compos Mater 2007;14:363–377. [CrossRef]

[10] Seemann R, Krause D. Numerical modelling of Nomex honeycomb sandwich cores at meso-scale level. Compos Struct 2017;159:702–718. [CrossRef]

[11] Seemann R, Krause D. Numerical modelling of nomex honeycomb cores for detailed analyses of sandwich panel joints. In: Oñate E, Oliver J, Huerta A, editors. 11th. World Congress on Computational Mechanics (WCCM2014) 5th. European Conference on Computational Mechanics (ECCM V) 6th. European Conference on Computational Fluid Dynamics (ECFD VI); 2014 July 20-25; Barcelona,Spain:Publisher;2014. pp. 2547–2558.

[12] Partovi Meran A, Toprak T, Muğan A. Numerical and experimental study of crashworthiness parameters of honeycomb structures. Thin-Walled Struct 2014;78:87–94. [CrossRef]

[13] Roy R, Park SJ, Kweon JH, Choi JH. Characterization of Nomex honeycomb core constituent material mechanical properties. Compos Struct 2014;117:255–266. [CrossRef]

[14] Xie S, Jing K, Zhou H, Liu X. Mechanical properties of Nomex honeycomb sandwich panels under dynamic impact. Compos Struct 2020;235:111814. [CrossRef]

[15] Waskom M, Botvinnik O, Hobson P, Halchenko Y, Lukauskas S, Warmenhoven J, et al. 2016, seaborn: v0.7.0 Available at: http://dx.doi.org/10.5281/zenodo.45133 Aceesed on Sept 20, 2020.

[16] SCHÜTZ, Cormaster C1 Technical Datasheet, Available at: https://www.schuetz-composites.net/downloads/datenblaetter/datenblatt-schuetz-cormaster-c1/datasheet-schuetz-cormaster-c1-en.pdf?cid=79c/ Aceesed on Sept 20, 2020.

[17] Tsujii Y, Tanaka K, Nishida Y. Analysis of mechanical properties of aramid honeycomb core (Investigation on the compression strength and the shear modulus). Trans Jpn Soc Mech Eng A 1995;61:1608–1614. [CrossRef]

[18] HEXCEL. HexWeb® Honeycomb attributes and properties. Avaliable at: https://www.hexcel.com/user_area/content_media/raw/HexWebHoneycombAttributesandProperties.pdf Accessed on Nov 02,2022.

[19] Nayak SK, Singh AK, Belegundu AD, Yen CF. Process for design optimization of honeycomb core sandwich panels for blast load mitigation. Struct Multidisc Optim 2013;47:749–763. [CrossRef]

[20] Jackson KE, Fasanella EL, Annett MS, Polanco MA. Material model evaluation of a composite honeycomb energy absorber. In: Oswald R,editor. 12th International LS-DYNA Users Conference; 2012

June 3-5; Dearborn, USA: Livermore Software Technology Corp; 2012. pp. 1–21.

[21] V. Gmbh, IVW - Schriftenreihe Band 77 Sebastian Heimbs Experimentelle und numerische Analyse des Schädigungsverhaltens kurzzeitdynamischer Belastung, n.d.

[22] LS-DYNA, Keyword User's Manual, Version 971, Livermore Software Technology Corporation, 2003.

[23] Minitab®. Getting started with minitab statistical software. Avaliable at: https://www.minitab.com/content/dam/www/en/uploadedfiles/documents/getting-started/MinitabGettingStarted_EN.pdf Accessed on Nov 03, 2022.

[24] Canonsburg TD. ANSYS Workbench User' s Guide. 2010;15317:724–746.

[25] Liu Q, Xu X, Ma J, Wang J, Shi Y, Hui D. Lateral crushing and bending responses of CFRP square tube filled with aluminum honeycomb. Compos B Eng 2017;118:104–115. [CrossRef]

[26] Yogeswaran R, Pitchipoo P. Characterization and machining analysis of AA3003 honeycomb sandwich. Mater Today: Proc 2020;28:4–7. [CrossRef]

[27] Xiao L, Song W, Xu X. Experimental study on the collapse behavior of graded Ti-6Al-4V micro-lattice structures printed by selective laser melting under high speed impact. Thin-Walled Struct 2020;155:106970. [CrossRef]

[28] Chen Y, Bai Z, Zhang L, Wang Y, Sun G, Cao L. Crashworthiness analysis of octagonal multi-cell tube with functionally graded thickness under multiple loading angles. Thin Walled Struct 2017;110:133–139. [CrossRef]

[29] Shu C, Zhao S, Hou S. Crashworthiness analysis of two-layered corrugated sandwich panels under crushing loading. Thin Walled Struct 2018;133:42–51. [CrossRef]

[30] Abdullahi HS, Gao S. A novel multi-cell square tubal structure based on Voronoi tessellation for enhanced crashworthiness. Thin-Walled Struct 2020;150:106690. [CrossRef]

[31] Menna C, Zinno A, Asprone D, Prota A. Numerical assessment of the impact behavior of honeycomb sandwich structures. Compos Struct 2013;106:326–339. [CrossRef]